LA-UR -88-160

CONF-880111--1

Los Alamos National Laboratory is operated by the University of California for the United States Department of Energy under contract W-7405-ENG-36.

TITLE: FRACTURE NETWORK MODELING OF A HOT DRY ROCK GEOTHERMAL RESERVOIR

LA-UR--88-160

DE88 005389

AUTHOR(S): Bruce A. Robinson ESS-4

SUBMITTED TO: 13th Workshop on Geothermal Reservoir Engineering
Stanford Geothermal Program
Stanford University
January 19-21, 1988

DISCLAIMER

Los Alamos Los Alamos National Laboratory
Los Alamos, New Mexico 87545

FORM NO. 836 R4
ST. NO. 2629 5/81

DISCLAIMER

FRACTURE NETWORK MODELING OF A HOT DRY ROCK GEOTHERMAL RESERVOIR

Bruce A. Robinson

Los Alamos National Laboratory
Los Alamos, New Mexico 87545

ABSTRACT

Fluid flow and tracer transport in a fractured Hot Dry Rock (HDR) geothermal reservoir are modeled using fracture network modeling techniques. The steady state pressure and flow fields are solved for a two-dimensional, interconnected network of fractures with no-flow outer boundaries and constant-pressure source and sink points to simulate wellbore-fracture intersections. The tracer response is simulated by particle tracking, which follows the progress of a representative sample of individual tracer molecules traveling through the network. Solute retardation due to matrix diffusion and sorption is handled easily with these particle tracking methods. Matrix diffusion is shown to have an important effect in many fractured geothermal reservoirs, including those in crystalline formations of relatively low matrix porosity. Pressure drop and tracer behavior are matched for a fractured HDR reservoir tested at Fenton Hill, NM.

INTRODUCTION AND MOTIVATIONS

Reservoir engineers and groundwater hydrologists have long recognized the importance of fractures on fluid flow and solute transport in underground porous media. Many analytical and numerical models exist to predict flow behavior for various fracture geometries ranging from a single fracture to multiple, interconnected fractures. Steady state or pressure transient responses can often be predicted using these models, which provide a macroscopic description of the flow process in terms of parameters suitable for use by hydrologists and engineers.

Solute transport is not so easily simulated using these models, however. The typical approach of employing the convective-dispersion equation with the adjustable parameter of dispersion coefficient usually fails in several important ways. In one dimension, a good match between model and field data is often difficult to achieve, since field data are seldom if ever perfect Gaussian distributions of residence times about a mean value. Multi-dimensional forms of the convective-dispersion equation can provide better fits, but at the expense of more adjustable parameters of questionable physical significance.

Fracture network modeling is a different approach to simulating flow and transport in fractured rock. The flow system is comprised of a network of interconnected fractures. A pressure difference imposed in such a system due to fluid injection or a natural hydraulic gradient results in a flow of water through the fractures. This flow field can be calculated assuming a fracture geometry, appropriate boundary conditions, and a relationship between pressure drop and flow rate within each fracture. Once the flow field is determined, the transport of a conservative, reacting, or adsorbing chemical component can be calculated using particle tracking techniques, which follow the progress of a representative sampling of tracer molecules through the network.

Fracture network modeling has been used extensively to model groundwater flow (see, for example, Castillo et al. (1972), Schwartz (1977), Smith and Schwartz (1980), Schwartz et al. (1983), Long et al. (1982), Andersson and Thunvik (1983), and Hopkirk et al. (1985), Long and Billaux (1987)). The primary focus of most previous work has been to determine the conditions under which a fractured rock could be treated as an equivalent porous medium. With the fracture network approach, one can assess the effect of fracture size, spacing, aperture, and orientation on the fluid flow, permeability distribution, and tracer behavior. Typically, Monte Carlo techniques are used, in which a large number of realizations of different fracture geometries, all with identical fracture statistics, are performed to determine the average and variability of behavior. The latter is a measure of the inherent uncertainty of flow behavior in the fracture network, given the measured statistical parameters. In most cases, these studies have assumed the flow to be within a rectangular grid in two dimensions, with constant-head boundary conditions at opposite ends of the plane and no-flow or linearly-

decreasing head boundaries on the two sides. These boundary conditions simplify the analysis and interpretation of results, and are probably sufficient for modeling large-scale groundwater flow problems.

Unfortunately, intervell flow and tracer tests in HDR geothermal reservoirs cannot be interpreted with these simplified boundary conditions. Wellbores often resemble point sources and sinks for flow, since they are directly connected to only a few fractures. In this study, we develop a code which realistically simulates the wellbore source-sink boundaries in fractured rock. The code is then used to model the fluid flow and transport processes in intervell flow and tracer experiments.

MODEL DEVELOPMENT

Fracture network modeling techniques are capable of handling many different model assumptions, such as regular or random fracture networks, a variety of boundary conditions and fluid flow laws, and various types of tracer transport processes. The model described below takes one set of assumptions which is particularly useful for HDR geothermal reservoir modeling.

Fracture Model Geometry: Figure 1 shows a two-dimensional fracture network containing two orthogonal fracture sets. Fractures are equally-spaced, and the average aperture of each set is known. Wellbores intersect the fracture network at the positions shown, and fluid is injected at constant pressure at one point and withdrawn at a lower pressure at a second point. The positions of the source and sink points and the numbers of each are adjustable. The outer boundaries of the square fracture network are assumed to be impermeable to fluid flow, as are the rock blocks between the fractures. A steady state flow field is set up within the fractures as a result of the constant-pressure and no-flow boundaries.

Fluid Flow Law: Assuming fracture flow can be modeled as laminar flow between parallel plates separated by distance w, the fracture aperture, the fluid velocity is given by

$$u = \frac{-w^2 \Delta P}{12 \mu L} \tag{1}$$

The volumetric flow rate per unit depth of fracture is

$$q = wu = \frac{-w^3 \Delta P}{12 \mu L} \tag{2}$$

The sign convention is such that flow into a node is positive, and flow from a node is negative.

Flow Equations: As noted by Castillo et al. (1972), the least number of unknowns results when an equation is developed for the pressure P at each node. Assuming steady state fracture flow with no pressure diffusion in the rock blocks,

$$\sum_{i=1}^{n} q_i = \sum_{i=1}^{n} \frac{w_i^3 (P_i - P_o)}{12 \mu L_i} = 0 \tag{3}$$

where n can be 2, 3, or 4, depending on the number of fractures connected to the node. Rearranging Eqn. (3):

$$P_o = \frac{\sum_{i=1}^{n} \frac{w_i^3 P_i}{L_i}}{\sum_{i=1}^{n} \frac{w_i^3}{L_i^3}} \tag{4}$$

where subscript o represents the node in question, and the i's refer to the adjacent nodes. Equation (4) is an expression for the pressure at node o in terms of pressures at each of the adjacent nodes.

Solution of Flow Equations: Equation (4) can be written for the pressure at each node, while the pressures of the source and sink nodes are set constant. The outer boundaries automatically simulate the no-flow condition because they are not connected to any points on the other side of the boundary. The resulting equation set is solved using the successive overrelaxation (SOR) method, an iterative solution procedure which offers a considerable improvement over the successive substitutions or Gauss-Seidel techniques. When the numerical parameter ω is optimized, the solution vector more rapidly approaches the correct values for slowly converging equation sets. A value of 1.87 was found to be optimum for a test problem, decreasing the number of iterations by a factor of 8.

Particle Tracking Technique: The assumption underlying the particle tracking technique is that a tracer response can be approximated by passing a large number of individual tracer molecules through the system, measuring the residence time of each, and accumulating the overall response, thus obtaining the residence time distribution of the individual molecules.

To calculate the residence time of an individual molecule traveling from the inlet to the outlet, the residence time within a fracture must be determined, and rules governing tracer transport at a node must be assumed. Within a fracture, tracer transport laws can be developed to account for dispersion, matrix diffusion, and adsorption. In the present study, we assume that dispersion within a fracture is negligible compared to overall dispersion levels measured in the fracture network (Robinson and Tester (1984)). Thus in the absence of

sorption or matrix diffusion, the particle residence time equals the fracture length divided by average fluid velocity, or, in terms of the variables used above:

$$\tau = \frac{-12\mu L^2}{w^2 \Delta P} \qquad (5)$$

Sorption and matrix diffusion are included by using the solution developed by Starr et al. (1985) for tracer transport in a single fracture. Tracer is assumed to travel in plug flow in the fracture and is transported by molecular diffusion to and from the stagnant fluid in the matrix. Adsorption can occur either on the face of the fracture or in the rock matrix. Assuming equilibrium adsorption with a linear isotherm in both the fracture and matrix, the tracer response at the outlet to a step change in concentration at the input is (Starr et al., 1985)

$$\frac{C}{C_{in}} = \text{erfc}\left[\frac{Di}{(\theta - R)^{1/2}}\right] \qquad (6)$$

where $\theta = t/\tau$ and Di, the diffusion number, is given by

$$Di = \frac{(D_{AB} R' \tau)^{1/2} \phi}{w} \qquad (7)$$

In the present study we will consider only conservative, nonadsorbing chemicals for which R and R', the retardation factors in the fracture and matrix, are equal to unity. Figure 2 shows the solution for values of Di ranging from 0.001 to 1. The step tracer response is equivalent to a probability distribution function for an individual tracer molecule. Thus, the residence time of a tracer particle in a single fracture is calculated stochastically by generating a random number between 0 and 1 and calculating the time corresponding to that value for C/C_{in} (see Figure 2). This methodology for simulating tracer transport processes in a single fracture is valid for any linear transport process, those for which the solution is independent of concentration.

At a fracture intersection, we assume complete mixing, whereby the tracer partitions to the different fractures in the same proportion as the flow rate. In the particle tracking formulation, the probability that an individual molecule at a node chooses a given fracture is equal to the flow fraction entering that fracture. A random number generator is used to choose which path a molecule takes. When the particle reaches the outlet port, the total residence time is sum of the residence times in the individual fractures.

When this calculation is repeated, say 10000 times, a distribution of residence times is obtained. To record the tracer response, a group of time blocks (0 to Δt, Δt to $2\Delta t$, $2\Delta t$ to $3\Delta t$ ...) are identified and the number of molecules with residence times falling in each of the time blocks is counted. The resulting histogram is the residence time distribution, equivalent to the response of the system to a short slug of tracer injected at the inlet. The integral of this function, when normalized to unity, is the cumulative residence time distribution F(t).

One additional complication is the effect of fracture roughness on the fluid flow and tracer transport laws. Although the parallel plate law has been used in the derivations given above, in reality the equivalent hydraulic aperture w_h is a weighted average value accounting for the distribution of apertures encountered by fluid passing through the fracture. This parameter is different than equivalent aperture encountered by tracer, w_t, and thus requires a revision of Eqns. (2) and (5). Due to the w^3 dependence on flow rate, the narrow apertures will contribute the most to the pressure drop. On the other hand, tracer molecules sample the entire flow volume and thus w_t is an unweighted average of apertures encountered in the flow path. Thus, the tracer aperture w_t will always be larger than w_h.

Long and Billaux (1987) addressed a similar issue in their study of data from the Fanay-Augeres uranium mine in France. Data were available from over 200 packer tests in which individual fractures were isolated and hydraulic conductivities were measured. In addition, the observed free aperture was measured in each case from examination of cores. Assuming the hydraulic aperture to be proportional to the free opening, Long and Billaux determined the average value for the ratio of hydraulic to free aperture to be 8.6. The free aperture is likely to be nearly equivalent to the tracer aperture w_t, since w_t is an unweighted mean of the true aperture distribution and the free aperture is determined from a core which randomly samples the aperture distribution of a fracture. Thus, we can expect potentially large differences between w_h and w_t. However, given that very little is known about this phenomenon, we will assume that w_h is proportional to w_t, but treat the ratio $f_w = w_t/w_h$ as an adjustable parameter. Thus, Eqns. (2) and (5) become

$$q = \frac{-w_t^3 \Delta P}{12\mu L f_w^3} \qquad (8)$$

and

$$\tau = \frac{-12\mu L^2 f_w^3}{w_t^2 \Delta P} \qquad (9)$$

In addition, the aperture in the definition of Di (Eqn. (7)) is w_t. Clearly, future theoretical and experimental research should be performed to aid in the understanding of the relationship of hydraulic and tracer apertures.

The computer code FRACNET was developed to solve for the steady state pressure field, flow patterns, and tracer behavior for the model summarized above. In addition, the code computes flow streamlines with a particle tracking technique.

The Fenton Hill Phase I Experiments

The Fenton Hill HDR program is designed to demonstrate the feasibility of creating and operating a prototype hot dry rock geothermal reservoir. In Phase I of the program, conducted in the 1970s, the feasibility of the concept was demonstrated in a series of hydraulic fracturing and flow tests (Dash et al., 1981). In the longest experiment, lasting 286 days, energy was extracted at an average rate of 3 MW thermal at a temperature of about 140°C. The present study focuses on hydraulic and tracer data obtained from this reservoir. Tracer response curves were measured by injecting a short pulse of irradiated NH_4Br^{82} salt dissolved in water and measuring the gamma activity as a function of time in the production fluid. Phase II of the program, which is designed to demonstrate the technology for long-term heat extraction on a larger scale at higher temperatures, is currently being carried out.

Results and Discussion

Table 1 lists the input parameters for the base case. Of these, the parameters which are fully or partially adjustable are f_w, the ratio of tracer aperture to hydraulic aperture, w_1 and w_2, the average tracer apertures for the two fracture sets, σ, the standard deviation of the aperture for the two fracture sets, the fracture spacing S, and the matrix porosity ϕ (used to evaluate tracer matrix diffusion effects). For the base case, agreement was achieved between the model and tracer data by using the measured value of ΔP and known physical property values, assuming the values of S, σ, and ϕ listed in Table 1, and adjusting the values of w_1, w_2, and f_w. To evaluate the "goodness-of-fit" of the simulation, three criteria were used: 1) the first arrival and peak tracer times must be matched; 2) the fraction of tracer recovered at the end of the tracer test (120 hr) should be within about 10% of the measured value of 0.83; and 3) there should be no anomalous behavior in the model results, such as multiple peaks, since the data have no such peaks.

Table 1 Input Parameters for the Base Case

N	40
L	300 m
S	25 m
ϕ	0
w_1	0.4 mm
w_2	0.4 mm
σ	0
f_w	2.36
P	2 MPa
D_{AB}	2.5×10^{-8} m^2/s
R	1
R'	1

A final consistency check on the model results requires the calculation of reservoir thickness. The flow rate per unit depth, q, at the injection or production well is calculated from Eqn. (8). The measured flow rate (6.31×10^{-3} m^3/s in this case) divided by q equals the reservoir thickness. If this thickness is less than the fracture spacing or much greater than the well spacing, then the model is utilizing an unrealistic reservoir geometry, even if the tracer data are reproduced accurately.

Base Case Results: For the base case, the inlet and outlet points were placed along the same fracture, as in Figure 1. Although f_w, w_1, and w_2 were adjustable parameters, it was found that keeping these values constant was adequate for all simulations presented in this paper. The calculated tracer pulse response is compared to the measured data in Figure 3. These curves are residence time distributions, normalized so that the area under the curves are equal to unity. The model results are plotted as a series of straight lines connecting the points in the residence time histogram. The first arrival and peak arrival times match the data reasonably well, and the fraction of tracer recovered at the end of the experiment, as measured by the area under the curves, are nearly equal for the two curves. Finally, although the curve exhibits some jaggedness, there is only one pronounced peak. The simulation meets the criteria established above, and thus is an adequate fit to the data. The integral of the pulse response curve representing the response to a step change in tracer concentration, is shown in Figure 4. The close agreement between model and data is more evident here because the integral smooths out the jaggedness of the pulse response curve.

The calculated reservoir thickness based on the model result and injection flow rate of 6.31×10^{-3} m^3/s is 48 m. Thus, the final consistency check on the model, that the reservoir simulation produce a reasonable 3-dimensional shape for the reservoir, is satisfied. This criterion is also met for the model results presented below.

The flow streamlines plotted in Figure 5 illustrate the nature of fluid flow in the fracture network. Much of the flow travels in a small region of rock near the injection and production points, but a significant fraction also travels in circuitous paths through a much larger region. This behavior gives rise to the observed tracer response consisting of an early, elevated concentration and a very long tail of the residence time distribution.

Effect of Fracture Spacing: In addition to the base case value of S=25 m, simulations were performed varying the fracture spacing while holding other parameter values constant. The flow geometries for these cases were similar to that of Figure 1, except that a larger fracture spacing results in fewer fracture intersections between the inlet and outlet points, and a smaller fracture spacing results in more fracture intersections. The resulting tracer response curves are shown in Figures 6a and b for S=15 m and S=50 m. The S=15 m case fits the data well, but the S=50 m case has too many individual peaks and thus fails to fit the data. With too few fracture intersections between the inlet and outlet, the reservoir with S=50 m does not contain a sufficient number of different possible routes for the fluid and tracer particles. The result is a tracer response curve with multiple peaks, in contrast to the smooth response curve measured. Thus the average fracture spacing of this reservoir is probably no greater than about 25 m.

Distribution of Fracture Apertures: In a fracture network, not all fractures have the same aperture. After extensive examination of fractures in cores, Snow (1970) showed that a lognormal distribution of apertures can be assumed. To simulate a fracture network with a lognormal aperture distribution, we randomly set the aperture value (subject to the lognormal distribution) for each flow segment in the network, treating each as an individual fracture. Figure 7 shows the tracer response for one realization assuming $\sigma = 0.5$ (units of ln(m)) for each fracture set (all other parameter values are those of the base case). The agreement is adequate, although one would have to perform more realizations to prove definitively that these model parameters with a distribution of apertures can be used to represent the Phase I reservoir. The flow streamline contour plot for this realization is shown in Figure 8. Fluid is diverted preferentially to fractures with larger apertures, resulting in distortions of the flow streamlines from the base case result of Figure 5. However, the correlation length for apertures is only 25 m, the fracture spacing. Since this value is much less than the well spacing, only the details of the flow field are affected by the distribution of apertures, while the overall tracer behavior is relatively unchanged. If large or small apertures were assumed to be continuous over longer distances, then the tracer behavior would have depended much more strongly on the distribution of apertures, and greater variability would be observed from one realization to the next.

Effect of Matrix Diffusion: Figure 9 shows the simulated tracer step response curves for different values of matrix porosity ϕ. Matrix diffusion exhibits a strong effect on the long-residence-time tail of the response curve, the effects becoming stronger for higher values of ϕ. The result is a decreased recovery of tracer for larger values of ϕ, as a larger fraction of the tracer is delayed in the stagnant matrix fluid.

Unfortunately, there exists no reliable technique for determining in situ matrix porosity in fractured granitic reservoirs, so a range from 0 to 0.005 was used. At the depths at which HDR reservoirs will typically be found, large earth stresses will compress the rock, lowering its porosity. However, injection of fluid at pressures nearly equivalent to the in situ earth stresses lowers the effective stress on the granite blocks, thus raising the porosity. Laboratory measurements of porosity on core specimens as a function of stress are possible, but in the process of recovering the core, the granite may have undergone additional fracturing as a result of cooling. The simulation just presented illustrates that matrix diffusion may have a significant impact on tracer behavior even in fractured granitic reservoirs, and that reliable techniques for measuring matrix porosity are needed to quantify this phenomenon.

Despite the uncertainties currently impeding progress, fracture network modeling holds great promise for characterizing fractured geothermal reservoirs. The approach used in the present study incorporates pressure drop and tracer data, two of the most common measurements in HDR reservoirs, into a physically realistic reservoir model. Thus, using currently available data, the model provides a better understanding of fluid flow and solute transport in fractured reservoirs. Furthermore, heat transfer can be included in the model to enable predictions of the thermal cooldown behavior to be made. Future work will extend the modeling to include heat transfer predictions.

CONCLUSIONS

1. A two-dimensional fracture network model has been developed to simulate steady state fluid flow and tracer transport in a two-well HDR geothermal reservoir.

2. Particle tracking techniques are used to simulate tracer advection, matrix diffusion,

and adsorption. Particle tracking can be used to model any linear transport process, one which is independent of tracer concentration.

3. Tracer data from the Fenton Hill Phase I reservoir is adequately simulated assuming a regular fracture network with fracture spacings of 25 m, apertures of all fractures equal to 0.4 mm, and f_w, the ratio of tracer to hydraulic aperture, equal to 2.36. Smaller fracture spacings also result in good fits to the data, but it is unlikely that larger values of S are realistic since they produce tracer response curves with multiple peaks not present in the field data. Imposing a distribution of aperture widths changes details of the flow field, but has little effect on the overall tracer behavior. Matrix diffusion can have a significant impact on tracer transport even in fractured granitic reservoirs.

4. Future research is required to constrain the fracture network model. The relationship between the hydraulic aperture, which is dominated by the smallest apertures in a rough fracture, and the tracer aperture, an unweighted mean of the aperture distribution, must be studied. Also, reliable techniques for estimating the in situ matrix porosity in fractured reservoirs are needed to quantify the effect on matrix diffusion on tracer transport.

NOMENCLATURE

C	tracer concentration (kg/m^3)
C_{in}	inlet tracer concentration during step input (kg/m^3)
D_{AB}	molecular diffusion coefficient of tracer (m^2/s)
Di	diffusion number (Eqn. (7))
$f(t)$	residence time distribution (s^{-1})
$F(t)$	cumulative residence time distribution
f_w	w_t/w_h
L	fracture length (m)
L_i	length of fracture i (m)
n	number of nodes connected to node o
N	number of rock blocks in each direction
P	pressure (Pa)
P_i	pressure at node i
P_o	pressure at node o
q	flow rate per unit depth (m^2/s)
q_i	flow rate per unit depth in fracture i (m^2/s)
R	tracer retardation factor in the fracture
R'	tracer retardation factor in the matrix
u	fluid flow velocity (m/s)
S	fracture spacing (m)
t	time (s)
w	fracture aperture (m)
w_1	average tracer aperture of fracture set 1 (m)
w_2	average tracer aperture of fracture set 2 (m)
w_h	hydraulic aperture (m)
w_i	aperture of fracture i (m)
w_t	tracer aperture (m)
ϕ	matrix porosity
θ	dimensionless time t/τ
μ	fluid viscosity (Pa-s)
ω	parameter in SOR solution technique
τ	fluid residence time in fracture (s)
σ	lognormal standard deviation of apertures (ln(m))

ACKNOWLEDGEMENTS

This work was performed under the auspices of the U. S. Department of Energy, Geothermal Technology Division. The author would like to thank Don Brown and Hugh Murphy for many useful discussions during the course of this work, and Cheryl Straub for helping to prepare the manuscript.

REFERENCES

Andersson, J., and R. Thunvik, Predicting Mass Transport in Discrete Fracture Networks With the Aid of Geometrical Field Data, Water Resour. Res., 22, 13, 1941-1950, 1986.

Castillo, E., Karadi, G. M., and R. J. Krizek, Unconfined Flow Through Jointed Rock, Water Res. Bull., 8, 2, 266-281, 1972.

Dash, Z. V. et al., Hot Dry Rock Geothermal Reservoir Testing: 1978 to 1980, J. Volcanology and Geothermal Res., 15, 59-99, 1981.

Hopkirk, R. J., Gilby, D. J, Rybach, L., and J. C. Griesser, Modelling of Heat and Mass Transfer in Deep, Fractured Crystalline Rock, Geothermics, 14, 2, 385-392, 1985.

Long, J. C. S., and D. M. Billaux, From Field Data to Fracture Network Modeling: An Example Incorporating Spatial Structure, Water Resour. Res., 23, 7, 1201-1216, 1987.

Long, J. C. S., Remer, J. S., Wilson, C. R., and P. A. Witherspoon, Porous Media Equivalents for Networks of Discontinuous Fractures, Water Resour. Res., 18, 3, 645-658, 1982.

Robinson, B. A., and J. W. Tester, Dispersed Fluid Flow in Fractured Reservoirs: An Analysis of Tracer-Determined Residence Time Distributions, J. Geophys. Res., 89, B12, 10374-10384, 1984.

Schwartz, F. W., Macroscopic Dispersion in Porous Media: The Controlling Factors, Water Resour. Res., 13, 4, 743-752, 1977.

Schwartz, F. W., Smith, L., and A. S. Crove, A Stochastic Analysis of Macroscopic Dispersion in Fractured Media, Water Resour. Res., 19, 5, 1253-1265 1983.

Smith, L., and F. W. Schwartz, Mass Transport 1. A Stochastic Analysis of Macroscopic Dispersion, Water Resour. Res., 16, 2, 303-313, 1980.

Snow, D. T., The Frequency and Apertures of Fractures in Rock, Int. J. Rock. Mech. Min. Sci., 7, 23-40, 1970.

Starr, R. C., Gillham, R. W., and E. A. Sudicky, Experimental Investigation of Solute Transport in Stratified Porous Media 2. The Reactive Case, Water Resour. Res., 21, 7, 1043-1050, 1985.

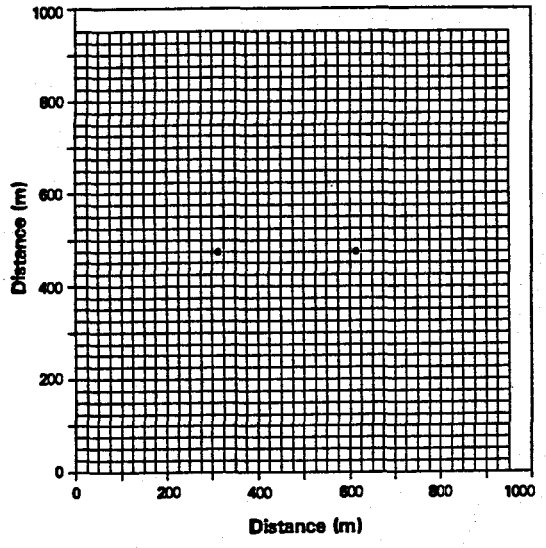

Figure 1. Typical fracture network with two fracture sets, inlet and outlet points, and outer boundary

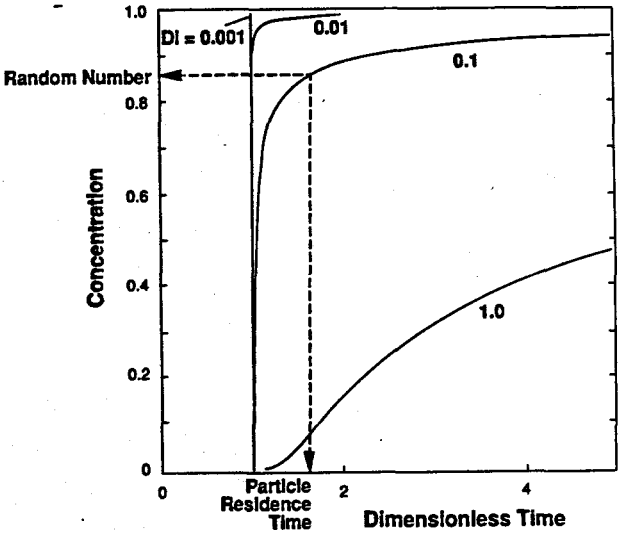

Figure 2. Tracer step response curves for flow through a single fracture with matrix diffusion for different values of the diffusion number Di. Also shown is a calculated value for residence time for a given random number.

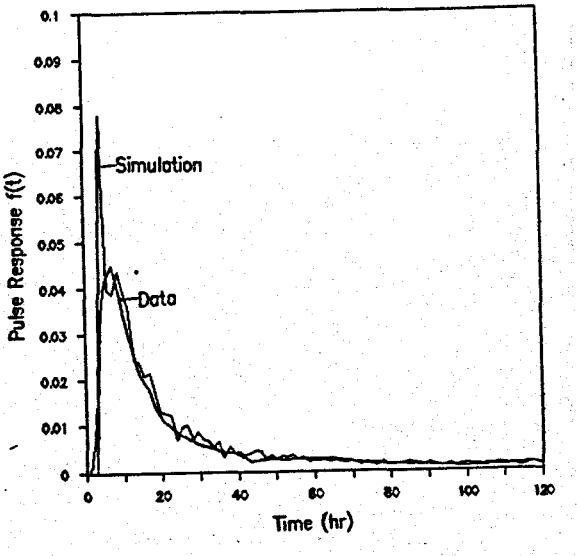

Figure 3. Comparison of measured and simulated pulse response curves for the base case.

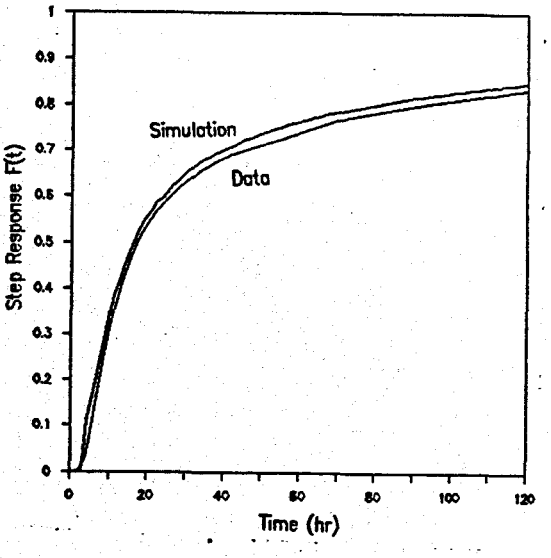

Figure 4. Comparison of measured and simulated step response curves for the base case.

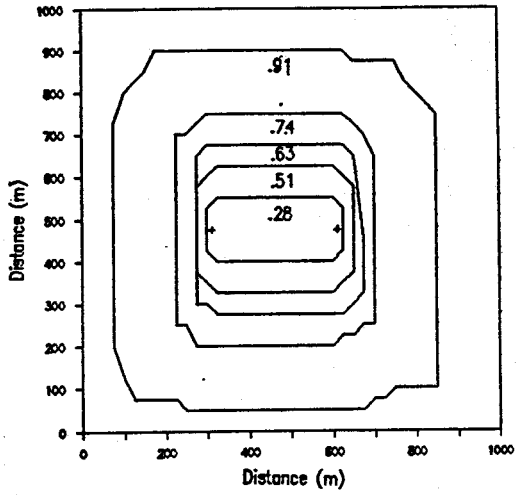

Figure 5. Flow streamlines for the base case.

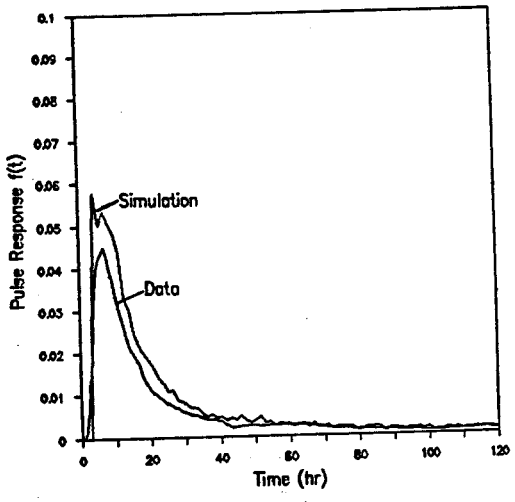

6 (a)

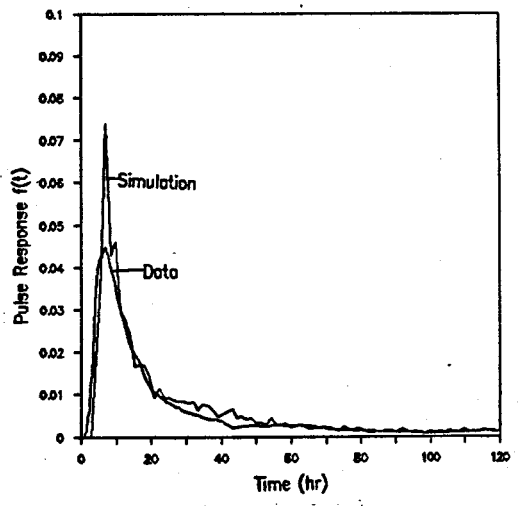

Figure 7. Pulse response for σ=0.5.

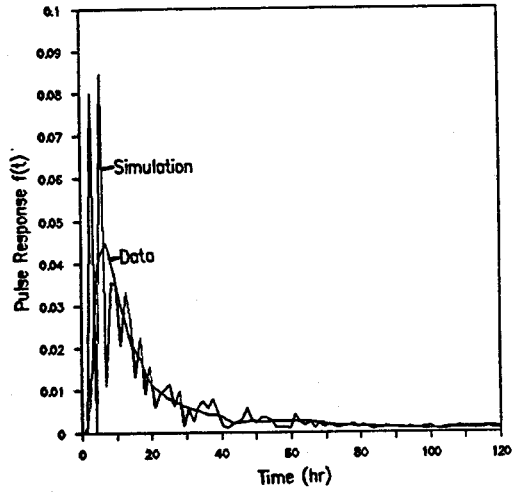

6 (b)

Figure 6. Pulse response curves for various values of S: (a) S=15 m; (b) S=50 m.

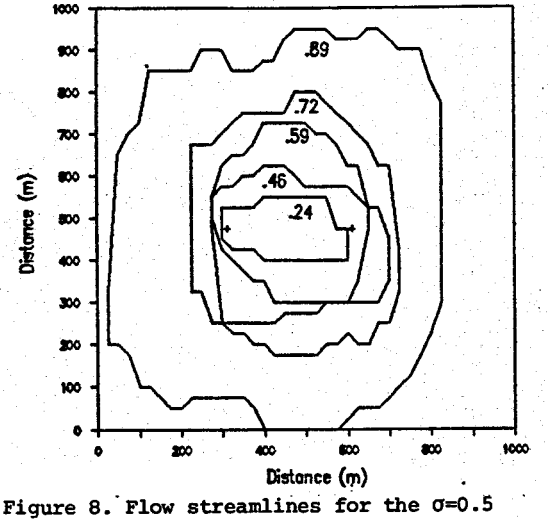

Figure 8. Flow streamlines for the σ=0.5 simulation.

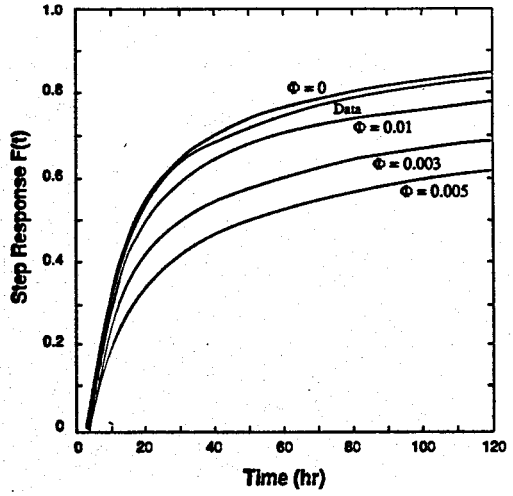

Figure 9. Effect of matrix diffusion: step responses for different values of ϕ.